Design and Control of a Synchronous Interleaved Boost Converter based on GaN FETs for PEM Fuel Cell Applications

Elie Togni, Frédéric Gustin, Daniel Hissel, Fabien Harel

ELECTRIMACS 2022 – Nancy, France, 16-19 May 2022

Design and Control of a Synchronous Interleaved Boost Converter based on GaN FETs for PEM Fuel Cell Applications

Elie Togni · Fabien Harel · Frédéric Gustin · Daniel Hissel

Abstract This paper shares some solutions in order to implement a state-of-the-art synchronous Interleaved Boost Converter (IBC), based on gallium nitride (GaN) power transistors. The solutions discussed have been implemented and validated on a synchronous 4-phase IBC (IBC4) prototype operating at a switching frequency of 250 kHz, specially designed to control the electric power delivered by a Proton Exchange Membrane (PEM) fuel cell module to a lithium battery pack. This paper focuses on digital control, such as PWM signal generation and the MCU requirements to reach high switching frequencies. It also discusses the issues related to the propagation delay of the sensors used and how to address them. The high switching frequency enabled by GaN transistors, combined with this DC/DC converter architecture and its phase-shifted control strategy, might heavily strain the load of the single MCU embedded. The real-time management of the different control loops is therefore exposed.

E. Togni · F. Gustin · D. Hissel
FEMTO-ST, FCLAB, Univ. Bourgogne Franche-Comté, CNRS
90010 Belfort cedex, France
e-mail: elie.togni@edu.univ-fcomte.fr,
frederic.gustin@univ-fcomte.fr, daniel.hissel@univ-fcomte.fr

F. Harel
Univ. Lyon, Univ. Eiffel, ENTPE, LICIT-ECO7, F-69675 Lyon
90010 Belfort cedex, France
e-mail: fabien.harel@univ-eiffel.fr

1 Introduction

Silicon, which has been adopted as the mainstream technology in power electronics over the last five decades, is now getting closer to its theoretical bounds [1]. Today, this material is widespread all around the world, especially inside integrated circuits and switch-mode power converters through MOSFETs, IGBTs and diodes components. Even if some improvements continue to be performed on existing products, manufacturers and researchers are leaning on better materials, such as wide bandgap (WBG) semiconductors for new power devices development. These materials are allowing smaller size devices to operate at higher switching frequencies, withstanding higher voltages and temperatures while having a lower on-resistance compared to silicon [2]. These outstanding intrinsic capabilities are leading to more efficient power conversion semiconductors, pushing further the enhancement in power electronics. Two promising technologies have emerged during the last decade and are already competing with previous ones: gallium nitride (GaN) and silicon carbide (SiC). Many electrical applications, such as power converters, variable-speed motor drives, LiDAR (Light Detection And Ranging), envelope tracking, audio amplifiers, or wireless power supplies arouse the interest of GaN semiconductors manufacturers [3]. However, literature and manufacturers rarely raise the opportunities to use GaN power semiconductors in fuel cell applications, while several of today's commercial products are showing well-suited characteristics for these applications. In the current context of search for more efficient energy solutions, fuel cells associated with new technology power electronics converters, such as GaN-based DC/DC converters, seems an interesting option to consider.

The remainder of the paper is structured as follows: section 2 brings a quick overview of the IBC4 prototype developed with GaN transistors, section 3 provides most of the technical solutions that have been implemented to control such a DC/DC converter, section 4 is dedicated to a reverse current protection and the paper ends with conclusions in the section 5.

2 IBC4 prototype overview

The objective of this work was to develop a prototype of a high-efficiency and highly compact DC/DC converter, suitable for a series hybrid PEM fuel cell system. The main function of this power converter was to ensure the transfer of electrical energy between a fuel cell module (composed of a stack of 80 cells and a nominal power of 3.3 kW) and a lithium battery pack of 120 V. The various theoretical, technical, and economic considerations have directed this research towards the development of a digitally controlled synchronous interleaved Boost converter (IBC), comprising four parallel elementary Boost power stages, whose switching cells have been made with latest-generation GaN transistors (ref. EPC2034C) from the American manufacturer EPC. Fig. 1 shows the developed prototype in the front of the PEM fuel cell stack.

Fig. 1 IBC4 prototype in front of an air-cooled 80-cell/ 3.3 kW open-cathode PEM fuel cell.

With heatsinks and fans, the converter occupies a volume of approximately 1.5 l for a mass of 650 g (i.e. a power density of approximately 2 kW/l and 5 kW/kg). The motherboard, which includes all the components measures 21 cm long and 16 cm wide, and the half-bridge boards are 3 cm high.

The digital control of the prototype was carried out using a dual-core microcontroller (ref. TMS320F28379D) clocked at 200 MHz. This microcontroller made possible the control of GaN transistors at a switching frequency of 250 kHz while performing various communication tasks through different protocols (I2C, SPI and CAN). In addition, a 90° phase shift of the control of each of the phases relative to each other has been implemented. This control strategy reduces the current ripple delivered by the fuel cell in addition to drastically reducing the size and the number of filter capacitors. The apparent frequency at the input and the output of the converter reached 1 Mhz.

This converter has been experimentally validated within an hybrid fuel cell system, composed of an air-cooled fuel cell module based on the previous stack of Fig. 1 and a lithium battery pack, as shown in Fig. 2:

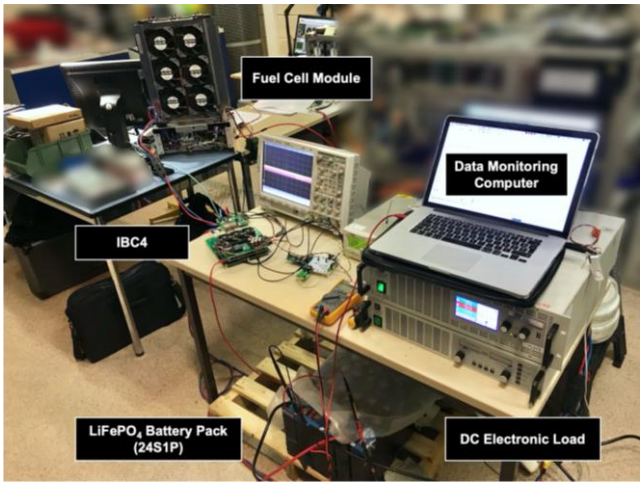

Fig. 2 Experimental setup used to validate the IBC4.

2.1. Synchronous IBC4 architecture

A simplified diagram of the synchronous IBC4 is depicted in Fig. 3:

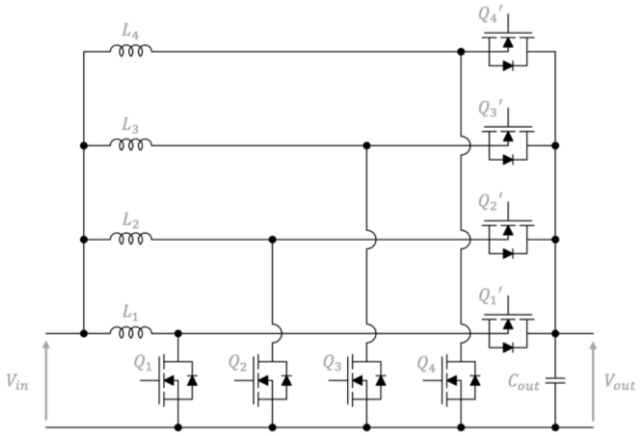

Fig. 3 Synchronous IBC4 simplified architecture.

2.2. Control architecture

The closed-loop control architecture of the IBC4 is depicted in Fig. 4. A first voltage loop is used to control the output voltage of the converter and set a limit equivalent to the maximum battery pack voltage. Four inner current loops are used to control the average current through each phase. Therefore, the current delivered by the fuel cell can be adjusted using the upper limit of the saturation block within the voltage loop.

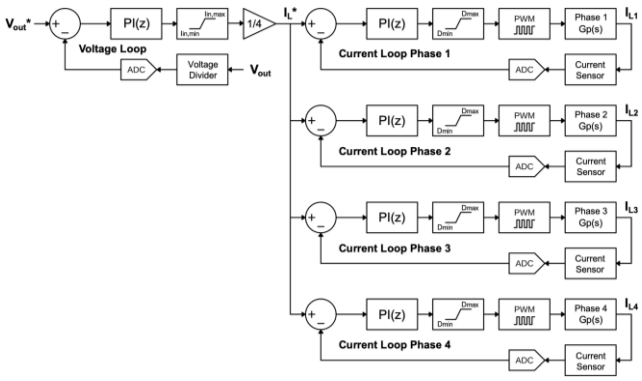

Fig. 4 Simplified cascade control loops.

3 Digital control considerations

3.1. Digital PWM signals generation

The eight PWM (dedicated to the control of the synchronous switching cells of the four phases of the IBC4 converter) were generated from four symmetrical triangular counters (Timer 1…4), synchronized and phase-shifted from one another by 90°, as depicted in Fig. 5. These counters have the advantage of enabling to center each of the PWM digital signals (PWM1A…4A) on the top of their respective counter, and to easily generate their complementary signals (PWM1B…4B).

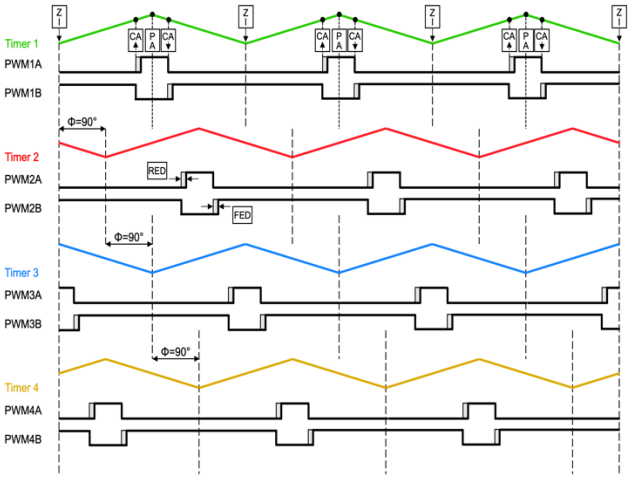

Fig. 5 PWM signals generation principle for controlling the four phases of the interleaved converter.

3.2. High Resolution PWM (HRPWM) signals

The control of a power converter at a switching frequency above 100 kHz may result in technical difficulties and the microcontroller in charge of controlling the power switches has to embed advanced PWM peripherals. Indeed, these signals must have a sufficient quantization resolution to avoid undesirable oscillations in steady state. One of the conditions for avoiding these phenomena requires that the resolution of the digital PWM signals be greater than the resolution of the ADC used to sample the signals from the electrical quantities to be regulated [4]. Unlike the resolution of an ADC which is fixed regardless of frequency, that of a PWM signal decreases as its frequency increases. To overcome this loss of resolution, one of the solutions consists in using counters with increased resolution. This enables the generation of high-resolution PWM signals (HRPWM), whose duty cycle can be adjusted with an accuracy of a few hundred picoseconds.

3.3. Sensors bandwidth and propagation delay

Theoretically, the current increases linearly in the inductor as long as the PWM signal controlling the low side transistor (PWM1A) is in the high state. As mentioned in the previous section, as long as the PWM signals are generated symmetrically with respect to the high value of the counter, synchronizing the measurement to this value should allow sampling the average current ($\overline{I_L}$) through the inductor, as depicted in Fig. 6:

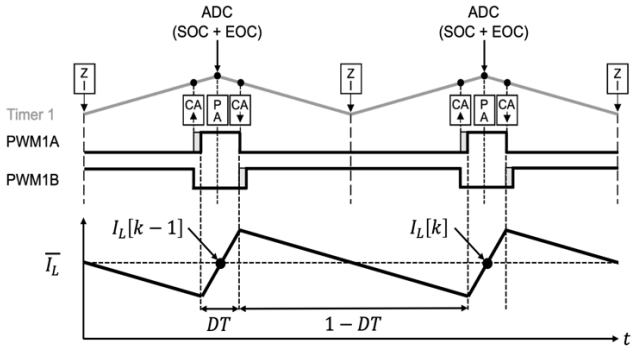

Fig. 6 ADC synchronization on the same timer used for PWM generation.

While voltage measurement at the input or output of a converter generally relies on a voltage divider, many techniques exist for current measurement [5]. In order to achieve the highest possible control bandwidth, current measurement requires the use of high-performance sensors with a bandwidth greater than the switching frequency. Also, these sensors must have a low propagation delay between their input and their output. Furthermore, depending on the location of these sensors in the power circuit, they may require high immunity to common-mode transients given the voltage variations (dV/dt) associated with the very fast switching times of GaN transistors [6].

During this work, isolation amplifiers (ref. AMC13x) have been used. These sensors have a high propagation delay (typically 2.5 µs) and a bandwidth below 300 kHz. Fig. 7, is a comparison between a high bandwidth oscilloscope current probe (C) (ref. Agilent 1147A) and a current feedback circuit based on this isolation amplifier (B) for a switching frequency of 250 kHz. (A) is the PWM signal controlling the low side FET of a Boost converter.

The solution applied consists in shifting the synchronization of the measurement to the peak of the next counter and extending the acquisition window duration of the ADC. This way, the signal is sampled about 2.5 µs later.

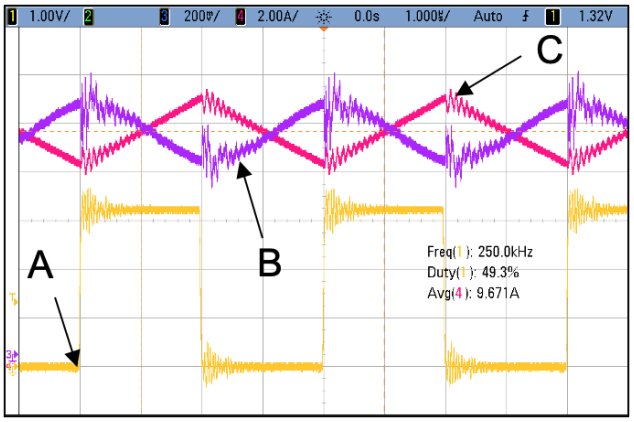

Fig. 7 Oscilloscope screenshot showing propagation delay and the effect of the bandwidth of an isolation amplifier (B) compared to a precision current probe (C).

3.4. Real-time management of critical tasks

One of the main difficulties encountered during the implementation of the control of the IBC4 converter was to ensure the execution of different tasks on a single microcontroller, in a time interval strongly constrained by the switching frequency and the phase shift of the PWM signals. Indeed, in order to maintain a maximum control bandwidth, the various control loops were synchronized on the four counters (Timer 1…4) used for the generation of the PWM signals (c.f. Fig. 5). Due to the high switching frequency targeted (i.e. 250 kHz) and the 90° phase shift of the control of the four phases relative to each other, the time available between two consecutive PWM signals was then reduced to one microsecond (1/1000 kHz). During this microsecond, the microcontroller has to perform critical control tasks (i.e. control loops), and also less critical tasks such as communication through different digital protocols (e.g. CAN, I2C, SPI…). During this work, it was found that if these tasks were performed on only one of the processors (CPU1 or CPU2) of the TMS320F28379D microcontroller, the CPU used was overloaded and unable to control the converter. To solve this, critical control tasks were implemented on its coprocessor (i.e. CLA1), thus reducing drastically the load on the associated processor (i.e. CPU1). The main interactions between the processor and its coprocessor are represented in the form of a simplified timing diagram in Fig. 8:

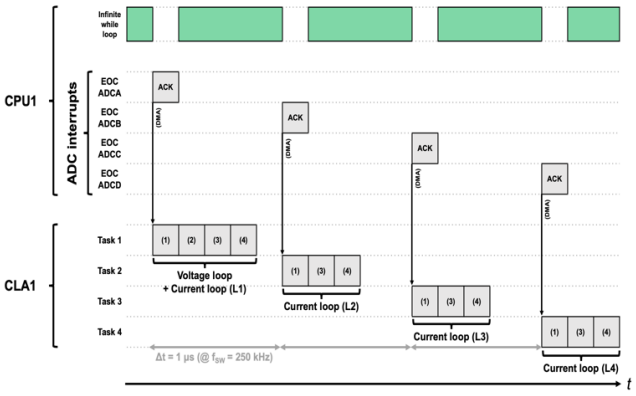

Fig. 8 Simplified timing diagram of the different tasks shared between CPU1 and its coprocessor CLA1.

In general, the control of the converter is based on various interrupts. Four ADC modules (ADCA…D) are synchronized to the high value of the four counters (Timer 1…4) used for the generation of the PWM control signals. The end of conversion (EOC) of each ADC module triggers both an interrupt in CPU1 (which is immediately acknowledged) as well as the execution of a task in CLA1 through a DMA (Direct Memory Access) module. Each task represented in Fig. 8 is then dedicated to the control of one phase of the converter and comprises up to four main steps exposed in Tab. 1.

Table 1 Main steps of the different tasks performed on the coprocessor for controlling the four phases of the IBC4

Step	Description	Phase 1	Phase 2	Phase 3	Phase 4
(1)	Read ADC EOC results	✓	✓	✓	✓
(2)	Compute output voltage compensator	✓	×	×	×
(3)	Compute phase current compensator	✓	✓	✓	✓
(4)	Update duty cycle	✓	✓	✓	✓

3.5. Digital compensator selection

Given this high switching frequency and the short time interval available between two successive PWMs (i.e. less than one microsecond), the use of a highly-optimized compensator structure programmed in assembly language has proven to be essential to ensure the correct execution of the various control loops. Therefore, a digital Proportional-Integral (PI) compensator structure from a specific library optimized for this microcontroller reference was used. The architecture is shown in Fig. 9, where $r(k)$ is the setpoint, $y(k)$ the measurement, and $u(k)$ the control effort.

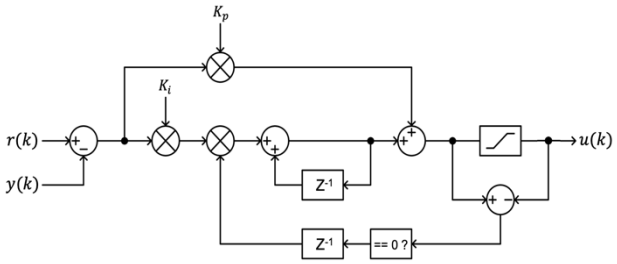

Fig. 9 Architecture of the digital PI compensator used.

This parallel architecture facilitates the tuning of the proportional K_p and integral K_i coefficients independently. The compensator output has a saturation block as well as an anti-windup allowing the integrator to be reset as soon as the high and low limits of the saturation block are reached. For the voltage control loop, this saturation block is used to adjust the limit on the current setpoint at the converter input. This setpoint is then divided by four and is used as a setpoint for the four average current control loops in each of the inductors of the four phases of the DC/DC. For the inner current control loops, this saturation limits the value of the duty cycle (typically between 0 and 90%). This PI compensator offers one of the best execution times, measured at 169 ns, between receiving input data and updating the control effort.

4 Reverse current protection in DCM

As mentioned above, the IBC4 converter consists of four elementary Boost converters connected in parallel which must ensure the transfer of electrical energy from the fuel cell to the battery pack. The use of synchronous switching cells implies that the converter can be bidirectional. Considering an elementary Boost converter, a reverse current may therefore be supplied from the battery pack to the fuel cell module through the high side transistor as illustrated in Fig. 10:

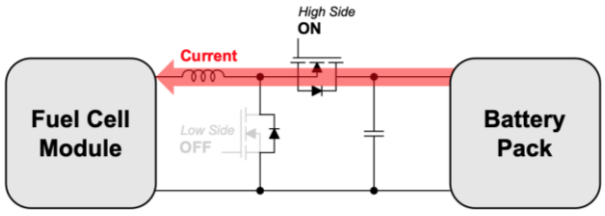

Fig. 10 Diagram illustrating a reverse current through the high side FET of a Boost converter.

Under non-fault condition, a Boost converter may operate according to three conduction modes, as long as the power supplied by the source increases. When it is started, the converter generally operates in discontinuous conduction mode (DCM), before transitorily operating in Boundary Conduction Mode (BCM), to finally operate in continuous conduction mode (CCM). Without any protection, a reverse current may occur when the converter operates in DCM.

4.1. Conduction mode detection algorithm

The simplest solution to avoid any reverse current would be to add a power Schottky diode at the input or output of the converter. However, this solution induces significant conduction losses (several tens of watts), when the fuel cell module operates at nominal power. With the objective of an electrical efficiency that must be as high as possible, another solution consists in implementing a control strategy to turn off the high side transistor, so that the latter operates only in reverse conduction (in a similar way to a diode) as long as the converter operates in DCM. Reference [7] caught our attention, presenting a method to detect the conduction regime of a synchronous boost converter. This method allows determining in real-time the conduction mode in which the converter operates and can easily be programmed on a microcontroller, without adding any electronic component. This article inspired the flowchart in Fig. 11, whose algorithm was programmed on the MCU of the IBC4 converter.

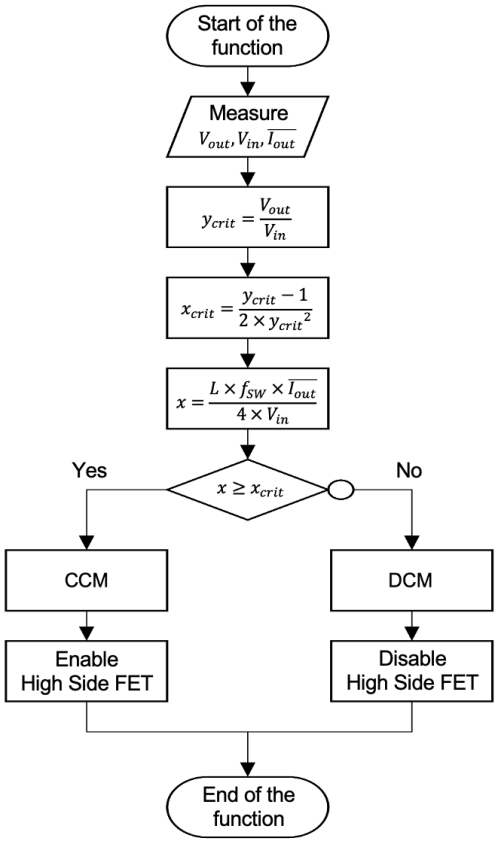

Fig. 11 Flowchart of the proposed conduction mode algorithm.

4.2. Gate drive considerations

As soon as the discontinuous conduction mode is detected, the microcontroller must disable the control of the high side transistors of the four phases of the IBC4 converter. A total of eight gate drivers (ref. UCC27611) were used to build the IBC4 converter (i.e. a single driver for each GaN transistor). These drivers incorporate an AND logic gate, which enables and disables the transmission of the PWM control signal, as shown in Fig. 12. Thus, as soon as the DCM is detected by the algorithm, the microcontroller can disable the high side drivers using four digital outputs, and activate them again when the converter operates in continuous conduction mode.

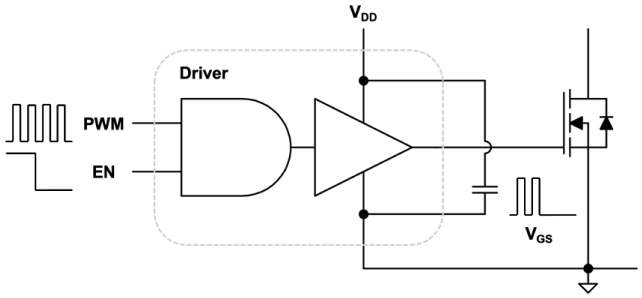

Fig. 12 Simplified diagram of a gate driver with an "Enable" input.

5 Conclusions

In this paper, some design and control considerations of an Interleaved Boost Converter based on GaN transistors are introduced. This research has highlighted the main challenges related to the use of GaN transistors in a power converter within a PEM fuel cell system. In addition, the use of synchronous switching cells involved the implementation of a functionality for detecting the discontinuous conduction mode (DCM). A digital solution without adding any component has been developed, thus avoiding any reverse current from the battery pack to the fuel cell module.

References

1. A. Lidow, "GaN as a displacement technology for silicon in power management," in 2011 IEEE Energy Conversion Congress and Exposition, Sep. 2011, pp. 1–6, doi: 10.1109/ECCE.2011.6063741.
2. J. Millan, P. Godignon, X. Perpina, A. Perez-Tomas, and J. Rebollo, "A Survey of Wide Bandgap Power Semiconductor Devices," IEEE Trans. Power Electron., vol. 29, no. 5, pp. 2155–2163, May 2014, doi: 10.1109/TPEL.2013.2268900.
3. A. Lidow, M. De Rooij, J. Strydom, D. Reusch, and J. Glaser, *GaN transistors for efficient power conversion*, Third edition. Hoboken, NJ: Wiley, 2020.
4. A. V. Peterchev and S. R. Sanders, "Quantization resolution and limit cycling in digitally controlled PWM converters," *IEEE Transactions on Power Electronics*, vol. 18, no. 1, pp. 301–308, Jan. 2003, doi: 10.1109/TPEL.2002.807092.
5. S. Ziegler, R. C. Woodward, H. H.-C. Iu, and L. J. Borle, "Current Sensing Techniques: A Review," *IEEE Sensors Journal*, vol. 9, no. 4, pp. 354–376, Apr. 2009, doi: 10.1109/JSEN.2009.2013914.
6. B. Liu, R. Ren, Z. Zhang, B. Guo, F. (Fred) Wang, and D. Costinett, "Impacts of High Frequency, High di/dt, dv/dt Environment on Sensing Quality of GaN Based Converters and Their Mitigation," *CPSS TPEA*, vol. 3, no. 4, pp. 301–312, Dec. 2018, doi: 10.24295/CPSSTPEA.2018.00030.
7. M. Kim, M. Shin, S. Choi, K. Bae, C. Won, and Y. Jung, "Reverse current control method of synchronous boost converter for fuel cell using a mode boundary detector," in *2014 IEEE International Conference on Industrial Technology (ICIT)*, Busan, South Korea, Feb. 2014, pp. 359–364. doi: 10.1109/ICIT.2014.6894869.